Starting nozzle flow simulation using K-G two-equation turbulence model

G.W. Yang, Z.M. Hu, and Z. Jiang

LHD Institute of Mechanics, Chinese Academy of Sciences,Beijing 100080, China

Abstract. The starting process of two-dimensional nozzle flows has been simulated with Euler, laminar and $k-g$ two-equation turbulence Navier-Stokes equations. The flow solver is based on a combination of LUSGS subiteration implicit method and five spatial discretized schemes, which are Roe, HLLE, MHLLE upwind schemes and AUSM+, AUSMPW schemes. In the paper, special attention is for the flow differences of the nozzle starting process obtained from different governing equations and different schemes. Two nozzle flows, previously investigated experimentally and numerically by other researchers, are chosen as our examples. The calculated results indicate the carbuncle phenomenon and unphysical oscillations appear more or less near a wall or behind strong shock wave except using HLLE scheme, and these unphysical phenomena become more seriously with the increase of Mach number. Comparing the turbulence calculation, inviscid solution cannot simulate the wall flow separation and the laminar solution shows some different flow characteristics in the regions of flow separation and near wall.

1 Introduction

For the development of high performance shock wind tunnel for hypersonic flow investigation and for the exhaust nozzle design of space vehicle engine, the nozzle starting process has been extensively investigated experimentally by Smith 1964, 1966, Amann 1969 and Saitio et al 1999, and numerically by Jacobs 1991, Chen et al 1994, Igra et al 1998, Saito et al 1999 and Mouronval et al 2002. For example, Amann (1969) experimentally studied the parameter influences of nozzle half-angle, throat width and nozzle inlet radius on the starting process. Igra et al (1998) and Mournval et al (2002) simulated the nozzle of Amann (1969) with 2-D plane and axisymmetric Euler Equations. Jacobs (1991) and Saito et al (1999) solved the laminar Navier-Stokes equation for the nozzle flow simulations. Concerning the rocket nozzle, Chen et al (1991) simulated the start-up and shut-down processes solving Navier-Stokes equation with the Baldwin-Lomax algebraic turbulence model.

In so far as the authors know, there is no any report about the simulation of nozzle starting processes with two-equation turbulence model. Most researchers believe the inviscid computations can predict satisfactorily the main flow features such as the primary and secondary shock waves, multiple shock wave reflections and slip surfaces. In fact, in the near region of nozzle throat, the flow may be separated, which can interact with the secondary shock, and the complete different flow phenomena may be produced if the wall flow separation is not simulated. For the nozzle flow of high Reynolds number, laminar assumption is virtually unreasonable, only turbulence calculation can predict the real interaction phenomena of separation flow and shock waves. In addition, for the complex internal flow calculation, multiblock grid is often used. The turbulence models, in common use, such as the algebraic Baldwin-Lomax (BL) (1978), the half-equation Johnson-King (JK) (1985) and the one-equation Spalart Allmaras (SA) (1992) models are all hard to apply to the blocks with no wall surfaces because these models need not only the local flowfield but also its corresponding gradient or distance values on the wall surface.

Two-equation turbulence models can overcome the shortcomings. The $k-\varepsilon$ turbulence model of Jones and Launder (1972) was extensively used for the calculation of incompressible flow. The $k-\omega$ turbulence model of Wilcox (1994) modified from the $k-\varepsilon$ turbulence model could be

used for high speed flows, which performs well for flows with adverse pressure gradients, but the behavior of ω close to solid boundaries makes it difficult to use for general aerodynamic flow problems, also, the model is very sensitive to the inflow values for ω. The $k-g$ model was improved by Kalitzin and Gould (1996) to overcome the shortcoming of the $k-\omega$ model. Up to now, $k-g$ model was mainly utilized for the calculations of external flows.

In the paper, for the simulation of the unsteady nozzle starting process, the $k-g$ two-equation turbulence model was added to the original implicit multiblock unsteady three-dimensional Navier-Stokes solver (containing BL turbulence model) implemented by the authors (2002, 2003). The spatial discretization in the original solver is Roe's FDS schemes, which contain the Roe upwind scheme (1981), HLLE scheme (1991) and the modified HLLE scheme (1994). For the comparison, the AUSM+ scheme (1996) and AUSMPW scheme (1998) have been completed recently for the solver. The purpose of the present work is to simulate the two-dimensional nozzle starting process. Two nozzle configurations studied by Amann (1969) and Saito et al (1999) have been considered.

2 Numerical method

In the study, the three-dimensional Navier-Stokes solver is used for the two-dimensional calculation. Three grid sections are enforced on the third dimension and the extrapolation of flow in the dimension is applied to guarantee the two-dimensional character of flowfield.

2.1 Governing equations

Using two-equation turbulence model, the flow governing equations are the well-known five time dependent Navier-Stokes equations added two $k-g$ turbulence model equations. In principle, this model could be implemented with the Navier-Stokes equations as a set of seven coupled equations, or the model could be a separate implementation that is decoupled from the Navier-Stokes equation. Considering our present objective is to simulate the unsteady starting process of nozzle, the fully coupled approach is chosen for the following calculation, even which would result in an increase in computational requirements.

2.2 Computational Scheme

In general, implicit schemes usually take much more CPU time to calculate at each time step than the typical explicit schemes, but they have high stability, therefore large time-step size can be chosen and the total CPU time is saved especially for the solution of unsteady Navier-Stokes equations. Of course, for the present study, the size of nozzle is smaller and the complex wave interaction needs to be solved. The time steps cannot be taken too large even if the scheme itself is unconditional stable. Therefore, implicit scheme may be not so efficient as the explicit schemes, but we still use the implicit time-marching schemes for our calculations.

Since $LU-SGS$ method of Yoon and Jameson (1988) can avoid the matrix inversion, its high efficiency makes the scheme extensively used for the simulation of steady flows. Unfortunately, the time-accuracy of the $LU-SGS$ scheme is less than the first-order, so the scheme is unsuitable for the time-accurate solution of the unsteady nozzle starting problems. Employing a Newton-like subiteration, second-order temporal accuracy can be obtained by utilizing three-point backward difference in the subiteration procedure. The numerical algorithm can be deduced as

$$\boldsymbol{L}\boldsymbol{D}^{-1}\boldsymbol{U}\Delta\boldsymbol{Q} = -\phi^{i}(1+\phi)\boldsymbol{Q}^{p} - (1-2\phi)\boldsymbol{Q}^{n} + \phi\boldsymbol{Q}^{n-1} + \boldsymbol{J}\Delta t * RHS, \tag{1}$$

here $\phi = 0.5$, and p is the subiteration number. The deduced subiteration scheme reverts to the standard $LU-SGS$ scheme for $\phi = 0$and $p = 1$. In fact, regardless of the temporal accuracy of the

left-hand side of Equation (1), second-order time accuracy is maintained when the subiteration number tends to infinity.

The viscous terms and the source terms in turbulence model are discretized by second-order central difference. The convective terms can be discretized by the following five spatial schemes. The first is the Roe scheme (1981), which is able to capture a shock and resolve the shear regions very accurately. Due to the violation of the entropy condition, unphysical numerical oscillation and carbuncle phenomenon often appear in the flow calculation at high Mach number. The second scheme is the HLLE scheme (1991), which is a modified version of Roe scheme. The scheme satisfies all of the stability, entropy, and positively conservative conditions required for the nonlinear difference equations. Compared with Roe scheme, the HLLE scheme introduces large numerical dissipation at contact discontinuities. A modified HLLE scheme was proposed by Obayashi and Wada [1994]. For the isentropic flow, the modified scheme results in the standard upwind-biased flux-difference splitting scheme of Roe, and as the jump in entropy becomes large in the flow, the scheme turns into the standard HLLE scheme, which has been successfully used for the subsonic, transonic and supersonic flow calculations. Since the calculated results of nozzle flow are strongly depended on the spatial schemes, ASUM+ scheme (1996) and AUSMPW (1998) are also completed for the comparison. At the middle Mach number, these two schemes can give the reasonable results, but unphysical oscillation and carbuncle phenomena reoccurs at high Mach number.

3 Results and discussion

3.1 Example 1

The first calculated example is the nozzle studied by Amann (1969), which also simulated by Mouronval et al (2002) by solving Euler Equations with WENO scheme and Runge-Kutta method at Mach numbers of 3 and 5.

In our numerical simulation, two grid blocks separated from the nozzle entrance is generated. The grid numbers in the two blocks are 100 × 100 and 600 × 100 respectively. For the initial and boundary conditions, it needs to be emphasized that the turbulence kinetic energy k and the turbulence parameter g are set as zero on the wall boundary. The inflow values of k and g are given as 3.75e-4 and 5.e-2 in present investigations, which is referenced the paper of Kalitzin et al (1996).

Through comparison of density contours of the Euler, laminar and turbulence calculations with the five schemes at Mach number of 3 shown in Fig. 1, Euler solutions of different schemes predict the same positions of primary shock (PS), secondary shock (PS) and contact discontinuity (CD). The main differences of different schemes appear in the region between the primary shock and the contact discontinuity. The results of Roe and MHLLE schemes exhibit carbuncle phenomena and numerical oscillation near the nozzle wall, which have also been found by many researchers. The present results of AUSM+ and AUSMPW schemes also show numerical oscillation near the wall, which corresponds with the analysis for AUSM+ but not for AUSMPW scheme by Kim et al (2002).The carbuncle phenomena and numerical oscillation near the wall still exist for the laminar and turbulence solutions, but its magnitude becomes smaller. The main differences between Euler and viscous solutions are in the region behind the secondary shock. Since the flow separation near the throat can be simulated by viscous calculation, the complex flow interaction of shock/vortex was well reflected in the viscous results. The density contours for turbulence calculations, however, are not very smoothly in the region behind the primary shock, which may be caused by the empirical coefficients in the $k-g$ two-equation turbulence model. Similar as the Euler and laminar calculations, the HLLE scheme is most robust and accurate for the nozzle flow.

The comparison of pressures along centerline of nozzle and on the wall with HLLE scheme is depicted in Fig. 2. The positions of the primary shock are agreement with each other, but the

secondary shock of Euler solution is much more afterward. Since Euler solution has no ability to simulate the flow separation behind the secondary shock, there is large difference in the region. The correspondence between the laminar and turbulence calculations is relatively well, but oscillating wall pressure was calculated in the flow separation region and behind the primary shock, it is indicated the stronger discrete vortex exist near the nozzle wall by the turbulence calculation.

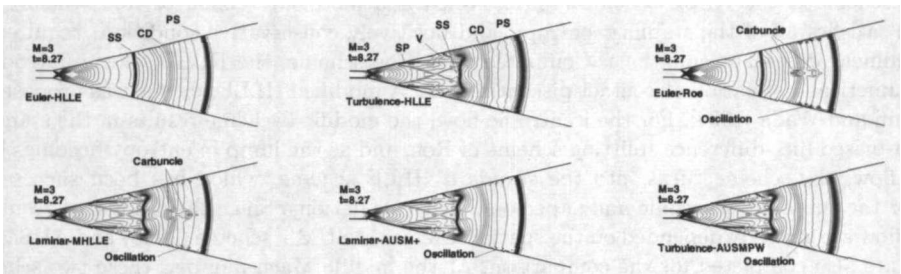

Fig. 1. Contours of density with five schemes at M=3 and nondimensional time of t=8.27

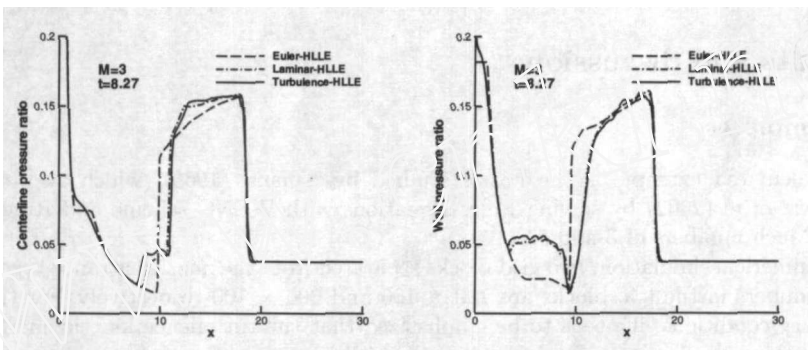

Fig. 2. Comparison of pressure on the wall and along centerline at M=3 and nondimensional time of t=8.27

For higher Mach number of 5, the carbuncle phenomena, oscillations and overshoots of pressure behind the primary shock occur for all schemes used except the HLLE scheme shown in Fig. 3. Even these schemes have been used extensively for the simulations of different flow problems, but for the hypersonic flows of nozzle, much effort to develop the spatial discretization methods having high accuracy, robustness and efficiency is still needed.

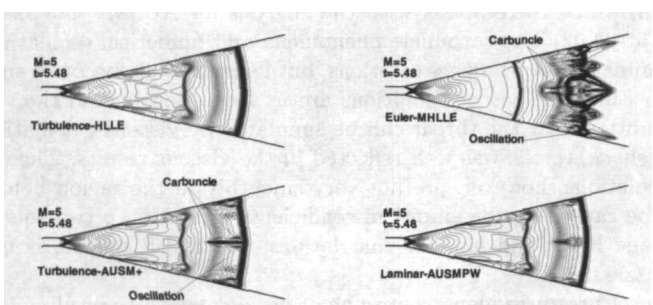

Fig. 3. Pressure contours for different schemes at M=5 and nondimensional time of t=5.48

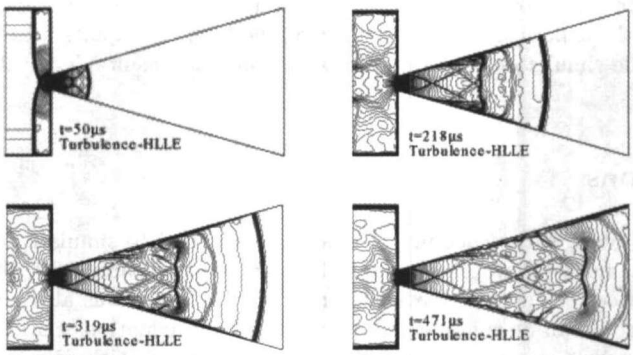

Fig. 4. Density contours of two-equation turbulence Navier-Stokes solution at M=2.5

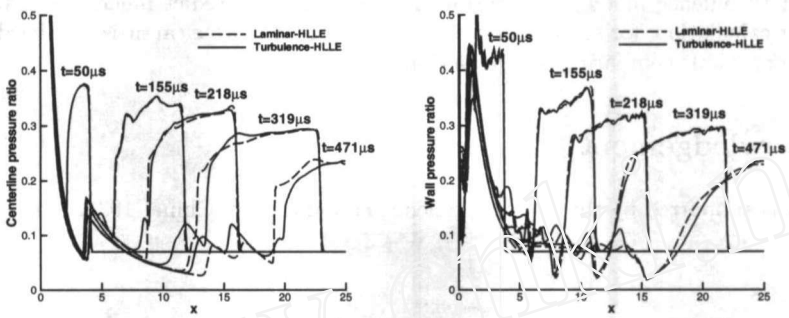

Fig. 5. Comparison of pressure on the wall and along centerline at M=2.5 and different nondimensional time

3.2 Example 2

Another example is the nozzle starting flow studied by Saito et al (1999) experimentally and numerically by solving laminar Navier-Stokes equations with single-block grid of 600x100. In present calculation, a multiblock grid with 3 blocks for the nozzle is generated, which contains 100×100, 100×100 and 600×100 grids, respectively.

Fig. 4 shows density contours of turbulence Naiver Stokes solutions at different times, respectively. On the arrival of incident shock wave, the primary shock wave (PS) at the nozzle throat continues to transmit in the main flow direction. The upper and lower parts are reflected at the shock-tube end wall, and then propagate back away from the wall and produce a stationary high- pressure region behind the upper and lower shocks, which result in two transverse shocks in the main flow and soon collide at the plane of symmetry and then transmit with each other. Due to the interaction between the transverse shock waves and the nozzle walls, the secondary shock (SS) and bubbles of boundary layer fluid are generated. Between the primary and secondary shock waves, a contact discontinuity (CD) following the primary shock is easily identified.

The main differences of laminar and turbulence solutions exhibit on the regions near wall and behind the secondary shock from the pressure distribution of Fig.5. The agreement between the present laminar result and Saito's laminar numerical results (1999) is quite good at all times. Even the present turbulence solution shows some different flow features comparing the laminar result, but which is not enough to compare with the experimental results. After 218s,

the numerically obtained flow field regardless of laminar and turbulence calculations starts to deviate from that the experiment. As stated above, the $k-g$ two-equation turbulence model was mainly used for the simulation of external flows, it may be unsuitable for the present internal calculation.

4 Conclusions

The $k-g$ two-equation turbulence model was complemented to simulate the starting process of two-dimensional nozzle flow. The numerical results are compared with the Euler and laminar results. The effect of different spatial discretization schemes was also investigated. Several important conclusions can be summarized: first, since Euler equations cannot simulate the separation flow, the nozzle starting process should be calculated with viscous solution. Second, for the nozzle flows of high Mach number, some schemes such as Roe, MHLLE, AUSM+ and AUSMPW may induce the unphysical oscillation and carbuncle phenomena. Third, due to the limitation of turbulence model, even turbulence solution can predict much reasonable results than laminar calculation, for some case such as the nozzle of Saito et al, it is still hard to obtain the satisfactory result comparing with experiment

5 Acknowledgement

This work was supported by the National Science Foundation in China, 10372106.

References

1. C.E. Smith: J. Fluid Mech. **24**, 625 (1966)
2. H.O. Amann: Phys. Fluids Supplement **12**, 150 (1969)
3. P.A. Jacobs: Simulation of transient flow in a shock tunnel and a high Mach number nozzle. NASA CR 187606 (1991)
4. C.L. Chen, S.L. Chakravarthy, C.M. Hung: AIAA Journal. **32**, 1836 (1994)
5. O. Igra, L. Wang, J. Falcovitz, H.O. Amann: Shock Waves **8**, 235 (1998)
6. T. Saito, K. Takayama: Shock Waves **9**, 73 (1999)
7. A.S. Mouronval, A. Hadjadj, A.N. Kudryavtsev, D. Vandromme: Shock Waves **12**, 403 (2002)
8. M.S. Liou: J. Comput. Phys. **129**, 364 (1996)
9. K.H. Kim and O.H. Rho: Comput. Fluids **27**, 311 (1998)